



Investigations on the Migration of Radiation-Induced Compounds in Polymeric Nuclear Track Detectors

Z. M. Badawy¹, M. F. Zaki² and E. K. Elmaghraby¹

¹ Experimental Nuclear Physics Department, Nuclear Research Center, Atomic Energy Authority, Cairo, Egypt

² Diagnostic Radiology Department, College of Applied Medical Sciences, Jazan University, KSA.

Received 18th Oct. 2017
Accepted 9th Jan. 2018

The late effect of radiation-induced modifications in polymeric material was investigated. The research focused on two morphologies of the polymer material, being either soft-optical structure or fibrous structures that represent a number of biological tissues and industrial materials. The aging effect was investigated by examining the formation of resin at the surface and within the fiber of the polymeric material. Micro-hardness test was used to investigate the surface of the PADC and Bayfol samples using the effect of indentation time. Optical microscope imaging was used to determine the extension of the organic resin on the surface of the PADC sample and to explain discrepancies in the hardness measurements. Polarizing optical microscope showed change in polarization in Bayfol samples as a result of indentation stress and with conjunction to radiation dose. Layers of radiation-induced compounds in poly-allyl diglycol carbonate (PADC) and intercalated synthesized compounds within Bayfol polymer fiber were found. Infrared absorption showed loss of free O-H groups of PADC samples and C=O group of Bayfol samples and prove that aromatic composition of Bayfol was more sensitive to radiation damage than aliphatic PADC composition. Results verified the aging effect and showed behaviors that reflect the action of radiation-induced modification long time after irradiation.

Keywords: Radiation damage/Micro-hardness/Ageing effect

Introduction

Synthesis of different substances during irradiation of polymers had been reported by our group [1-4]. The main product is water-free molecules, carbon oxides and alcoholic compounds with OH⁻ group attached to scissor chain radical [5-7]. The processes of formation of organic compounds in irradiated samples are associated with the chain scissoring, re-polymerization and cross linking and atomic displacements [1,2,8,9]. Time evolution of irradiation-induced modification on nuclear track detectors, such as polyallyl diglycol carbonate (PADC) and Bayfol is a slow process due to trapping of irradiation induced compounds inside the bulk material. In the present work, migration of these compounds will be investigated. This work

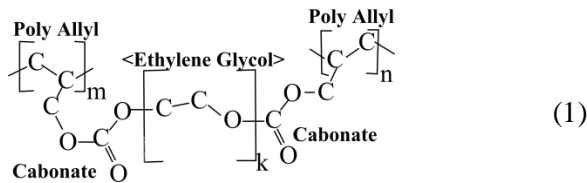
focused on the Vicker's micro-hardness measurements, which are used to study the effect of irradiation on the mechanical properties of these polymers together with the surface and bulk morphology. Infrared absorption was to track the change at the molecular scale.

MATERIALS AND METHODS

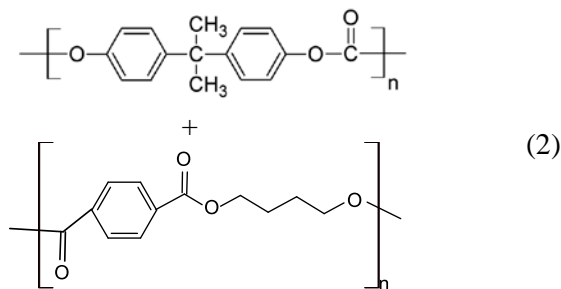
Materials

Two materials (poly allyl diglycol carbonate and Bayfol) were chosen because of the difference in their bulk morphology and chemical composition (PADC is an aliphatic compound while Bayfol contains cyclic aromatic groups). Additionally, both of them have effective use as a nuclear track detector and optical material. PADC is one of the trade names of the family of Solid State Nuclear

Track Detectors. The chemical composition of PADC is $(C_{12}H_{18}O_7)_n$,



PADC has density of 1.32 g/cm^3 . PADC sheets, used in this study, were manufactured by Track Analysis Systems Ltd. The sizes of specimen's were $1 \text{ cm} \times 1 \text{ cm}$ and 2 mm thickness. The second one is Bayfol CR 1-4 polycarbonate blend with overall chemical composition of $(C_{16}H_{14}O_3)_n$. It is extrusion film based on Makrolon polycarbonates (PC) and polybutylene terephthalate (PBT) blend [10],



Bayfol is manufactured by Bayer (Leverkusen, Germany), specimen size was $1 \text{ cm} \times 1 \text{ cm}$ with an average thickness of $375 \mu\text{m}$ and density 1.23 g/cm^3 . The two materials represent the morphological structure of considerable fraction of biological tissues and industrial materials.

Irradiation

Samples were irradiated by the ^{60}Co gamma-ray irradiator at Inshas Cyclotron Facility, Atomic Energy Authority, Cairo, Egypt, during year 2010 with dose rate ranging from 1.8 kGy/h at the end of the irradiation to 2 kGy/h at the beginning of irradiation.

Indentation

Vickers micro-hardness test involves forcing a diamond pyramidal indenter into the surface of the material being tested. After indenter removal, indentations are being determined using usual light microscope. A calibrated machine (Shimadzu Model HMV-2000 micro-hardness tester) was

used to force a diamond indenter into the surface of the material being evaluated. The measurements are done in few minutes after indentation; so it is assumed that the indentation does not undergo elastic recovery after force removal. The indentation was done at room temperature. The appreciated indenting load chosen was 0.5 kgf after several tests. For each sample, the duration of indentation was swapped from 5 s to 60 s time. Statistics was obtained from, at least, three measurements at different locations on the sample surface. The Vicker's Pyramid Number (HV) was determined from the relation [11]

$$HV = 1.8544 \frac{F}{d^2}, \quad (3)$$

where F is the load in kgf , d is the average diameter of the two diagonals of the pyramidal shape in mm .

There was a difficulty in determining the diameter of the two diagonals of the pyramidal shape associated with the transparency of samples. To overcome such difficulty, the samples were illuminated by light emitting diodes from the perpendicular side to the axis of the optical microscope. Such setup enables identification of the edges of the pyramidal shape as a result of internal reflection. The material was tested for visco-elastic recovery of indentation 1 h after indentation, and no significant difference was observed.

Results and Discussion

Optical microscope study

Samples were examined under the optical microscope for any surface alteration within 15 days after irradiation. This earlier examination did not give a significant difference among irradiated sample. However, samples, after seven years of preservation in dark safe, showed microscopic formation of resin on the surface of the PADC samples. This resin had adhered to the surface and forms islands and extended layers of few-micrometer thickness. The expansion of these layers increased with the original dose to which it was exposed.

For PADC, the possible source of formation of the resin layer is the migration of synthesized compounds from the interior of the sample to the surface during the preservation time (7 years). During such period, compounds with small

molecular weight migrate *through* the material, together with reaction of synthesized compounds with each other and with water-free and hydrogen gas; such time evolution is yielding additional class of radiation induced effects in the material, the *aging effect*. The migration to the surface of PADC samples had formed the resin which covers the surface in part or as a whole depending on the dose. Figure (1) shows the optical microscope image of these extensions on PADC samples at different doses. For low doses, the expansion of the resin on the surface is limited, forming unconnected islands of the resin; while at high exposure dose, resin covers the whole surface with thick layer.

Surface morphology of Bayfol samples were difficult to manage, as it contains fibrous structure; so compounds migration may occur inside the bulk material beside the surface of these fibers. A special technique was used to photograph the surface; it is based on the change in light polarization passing through the polymer. The stress on the polymer, due to indentation, should be distributed through the material causing a change on the polarization angle of light. Two linear polarizing sheets were placed before the sample optical set and after the objective optical set. The polarizing angle was set to 90° between them, see Fig.(2) Lens curvature contributes also to the change of the plane of polarization. However, this change is homogenous and symmetric and it affects only to the brightness of the image. The image was recorded using a CMOS CCD camera with auto-focus function.

Three absorption filters were used to filter the light from the source as shown in Fig. (2); the Red filter at wave length 600 nm, the Green filter at wave length 555 nm and the Blue filter at a wave length 420 nm. Images were recorded with white light and with the three filters and the results are illustrated in Fig. (3) as a tabular figure. The scale bare is accurate within 5% of the originally determined scale due to the consequence of auto-focus function of the camera.

The white light images (Figs. 3 *a1,b1,c1,d1*) did not reveal visual alteration made by irradiation on the Bayfol. Images of the pristine sample, using polarized light and red filter (Fig. 3 *a2*), showed a change in the polarization in the volume around the indented *corners* of the Viker pyramid; with the Green filter (Fig. 3 *a3*) the same change in

polarization persists but with less strength, the strength of change in polarization is reduced further in the blue light range (Fig. 3 *a4*.)

The irradiated sample, on the other hand, showed a continuous increase in the strength of changing polarization. The volume affected by indentation was enlarged continuously to involve a volume around the *edges* of the pyramid for samples irradiated with 500 kGy (Fig. 3 *b2*) and 1050 kGy (Fig. 3 *c2*); and to involve all the volume around *faces* of Viker pyramid for the samples irradiated with a dose of 1950 kGy (Fig. 3 *d2*.) Such change in polarization could not be detected in PADC samples. To explain the difference, the morphology of these two polymers must be taken into account. Unlike the solid bulk of PADC which forces the synthesized compounds to migrate to the surface of the sample, the fibrous morphology of Bayfol may exploit the available room around fibers. Increasing radiation dose, initially delivered to the samples, should increase the amount of synthesized compounds as depicted from previous work [1,12]; the synthesized compounds fills spaces among Bayfol fibers; as a result, the indentation stress, which is the reason of change in polarization, will spread in more volume around the Viker pyramid beginning from corners in case of the pristine samples, then edges, up to the volume around faces, as mentioned before. The strength of polarization change was reduced with changing wavelength from 600 nm (Fig. 3 *raw 2*) to 420 nm (Fig. 3 *raw 4*) give a clue about formation of chiral molecules with circular dichroism property.

Micro-hardness study

The indentation time versus micro-hardness values of the specimens are shown in Fig. (4) for PADC, and Fig.(5) for the Bayfol, and for different primary doses. The PADC pristine sample shows the curve for time effect on the Vicker indentation similar to that of visco-plastic polymeric material in which the indentation diameter increases with indentation time due to the plasticity of the polymer. However, for small indentation time, the size of indentation may be slightly changed after indentation; i.e. recovered during the time needed for measuring indentation lengths; hence pristine samples may, apparently, show more hardness with small indentation time. Indentation time as long as 45 s, creates steady plastic deformation needed for precise determination of micro-hardness.

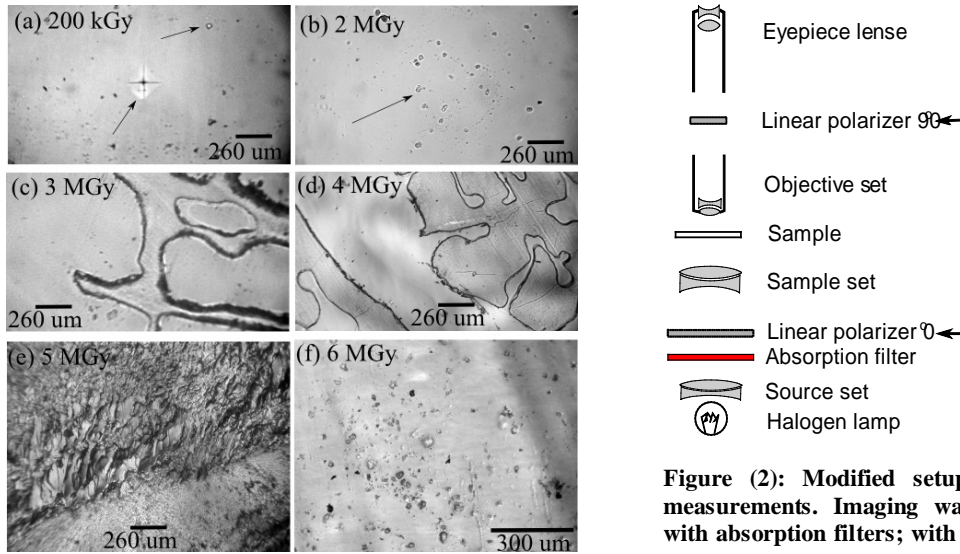


Figure (1): Optical microscope image of resin extension on the surface of PADC samples at different doses. The embryo of the resin begins to appear at doses of 200 kGy and spread out through the surface of the samples as the dose increase. At 6 MGy dose, the resin covers most of the surface of the sample. The scale bar may vary within 5% due to the auto-focus function of the CMOS CCD camera.

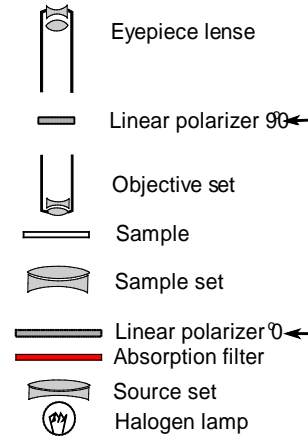


Figure (2): Modified setup for the polarized light measurements. Imaging was performed without and with absorption filters; with Red ($\lambda = 600$ nm), Green ($\lambda = 555$ nm), and Blue ($\lambda = 420$ nm)

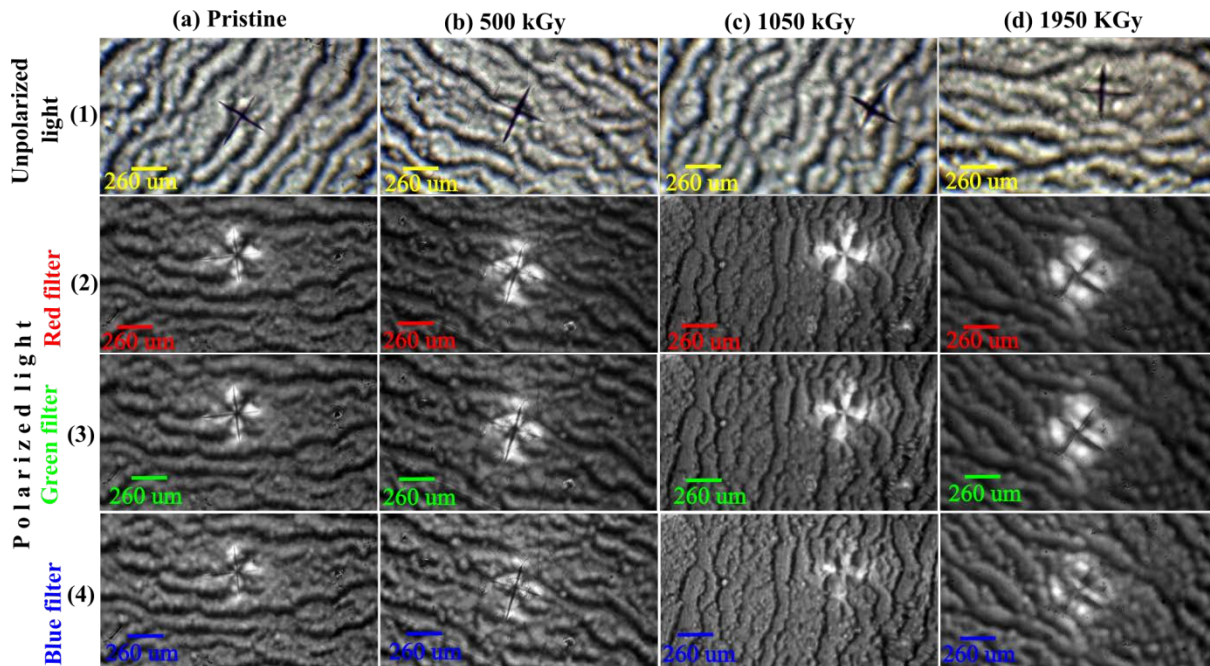


Figure 3: Polarized and unpolarized light optical microscope images for Bayfol samples at different doses. The scale bar may change within 5%.

For samples exposed "originally" to higher doses, the material hardens so that the indentation time has a slight effect on the resulting size of pyramid. The position of the indentation on the other hand increases the uncertainty in the diameter. If the indenter fall within portion (area) of the sample that is covered with resin, it forms a larger indentation and gives a lower value of HV; "apparent value". Consequently, for larger indentation time, the indenter bypasses the layer of soft resin and reaches harder material of the sample. Both effects make the curve of indentation time-dependent micro-hardness more flatten, this is obvious for PADC samples exposed to 50 Gy, 1 k Gy, 500 k Gy, as illustrated in Fig. (4). Hardening of polymer with dose was reported by many researchers [13,14].

The samples irradiated with 3 MGy dose had high uncertainty, especially at a small indentation time, because of the resin in the surface is of a non-uniform thickness. Additionally, the indenter may not reach the original surface of the sample; giving only the HV value of the resin, not the bulk material. The HV, for 3 MGy PADC sample, seems to be increased with time from 5 to 15 s indentation time and decreases afterward. For longer indentation times, samples seem to be softer than the bulk of the irradiated material but harder than the pristine PADC sample itself. This observable behavior may be attributed to migration of softer synthesized compounds to the surface of the resin layer itself, leaving much softer layer of a type of compounds on the layer of harder resin layers.

A different behavior was pronounced for Bayfol samples as illustrated in Fig. (5) Which shows that there is no noticeable variation between irradiated samples and the pristine sample. However, the texture of the Bayfol causes large uncertainty in the measurement of indentation diameter and consequently the value of HV. As for the previous results of polarizing optical microscopy, migration of synthesized compounds may take place within the fiber of Bayfol, especially at low doses. For 1 MGy dose, Bayfol showed behavior similar to PADC samples irradiated with 3 MGy; i.e. HV is being increased with time of indentation from 5 s to 15 s. However, this behavior cannot be ascribed to

inter-layer migration of the softer synthesized compounds but rather be associated with the loosely connected fibers on the surface of the sample.

The overall variation of micro-hardness with the original exposed dose is illustrated in Fig.(6). The force and indentation time are the same as previous measurement. Several additional samples of PADC were measured to cover the range of doses from 0 to 5 MGy. Quite a few identified domains of doses are illustrated.

The first domain is from 0 to 1 kGy, in which the material hardens at the beginning of irradiation. As illustrated above, a smaller amount of resin is formed and migrated to the PADC surface during the aging process. The second stage is associated with the decomposition and chain scissoring from 1 kGy to 50 kGy. Chain scissoring, on the other hand, competes the governing repolymerization and cross linking at higher doses up to about 500 kGy. Cross linking at this range of doses is attributed to existence of active polymer chains. The forth domain is associated with the domination of radiation-induced synthesis; a large number of unpolymerizable compounds are released; which extend to the 5 MGy dose. Part of this domain, fifth one, is attributed to full coverage of the sample surface with the synthesized resins.

Infrared results

Samples were investigated, non-destructively, by inferred spectroscopy (i.e. without mixing them with KBr, as usually done in FTIR). In Fig. (7a), three infrared absorption spectra of PADC samples, are illustrated in the wavenumber range 1300–3700 cm⁻¹; specifically, pristine sample, a sample just irradiated with 1 MGy dose, and sample irradiated with 1 MGy dose and aged for 7 years. Here, α_{sample} is the linear absorption coefficient determined as

$$\alpha_{sample} = \frac{1}{t_{sample}} \ln \frac{100}{T\%} \quad [mm^{-1}] \quad (4)$$

Where t_{sample} is the sample thickness in mm, and T% is the percentile transmittance at the specific wave number, k .

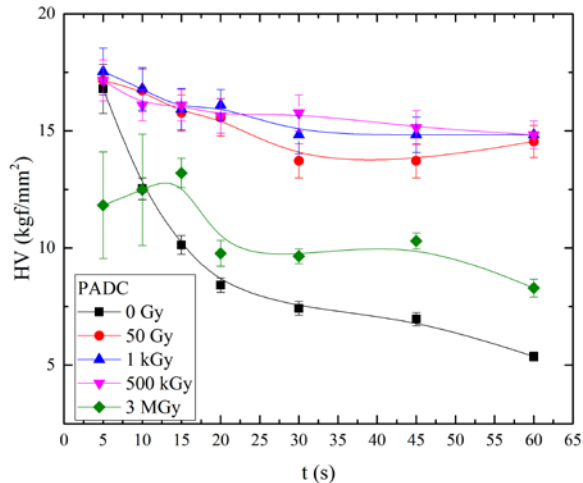


Figure (4): Indentation time-dependent micro-hardness values of PADC for samples irradiated with different doses

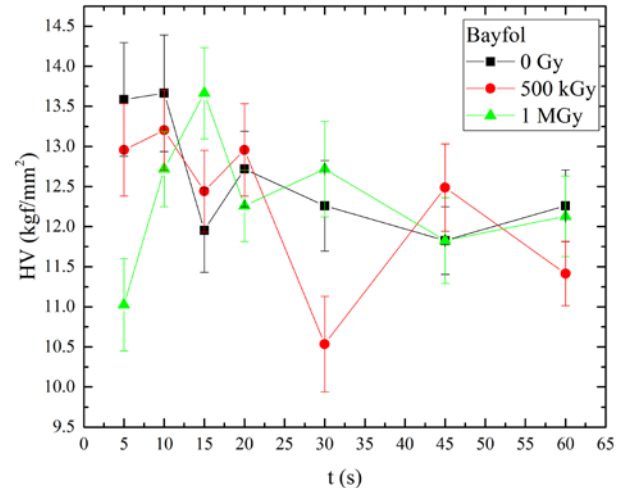


Figure (5): Indentation time-dependent micro-hardness values of Bayfol for samples irradiated with different doses.

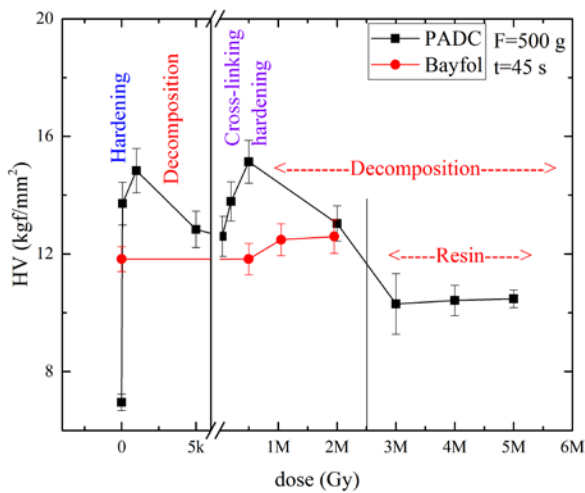


Figure (6): The variation of HV with dose for PADC and Bayfol nuclear track detectors.

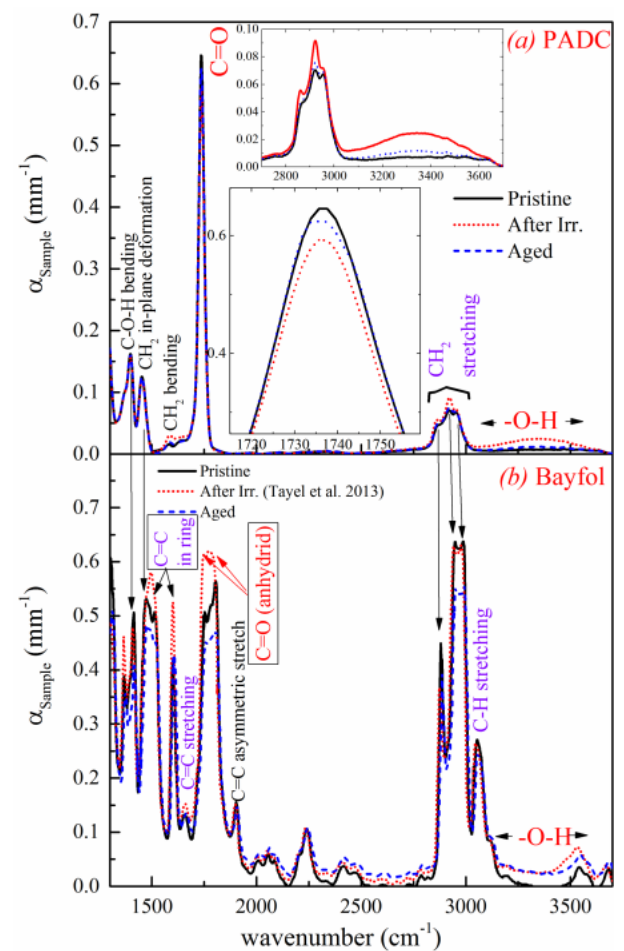


Figure (7): Infrared absorption spectra for pristine sample, sample irradiated with 1 MGy dose, and sample irradiated with 1 MGy dose and aged for 7 years. Material represented in part (a) is polyallyl diglycol carbonate and in part (b) is Bayfol CR

The common absorption peaks in both materials are the 2971 cm^{-1} , 2941 cm^{-1} and 2875 cm^{-1} absorptions which mark for asymmetric CH_2 stretching, asymmetric C-H stretching, and symmetric C-H stretching, respectively. The two absorption at 1598 cm^{-1} and 1514 cm^{-1} may be related to either C=C stretching in aromatic rings of Bayfol or to symmetric and antisymmetric vibrations of two carbonyl groups in attachment to same PADC molecule. The 1459 cm^{-1} absorption peak is related to CH_2 in-plane vibration. The C-O-H bending vibration is noticed at 1392 cm^{-1} . Specifically Bayfol samples showed absorptions at 3115 cm^{-1} and 3052 cm^{-1} which is related to C-H stretching in aromatic ring; the complete identification of Bayfol CR absorption peaks is in Ref. [8].

Two particular groups are of significance to our discussion, the C=O and free O-H groups. In PADC, the C=O absorption is pronounced at 1736 cm^{-1} . No signature for the broad free -O-H vibration around 3300 cm^{-1} was found in the pristine sample. Just after irradiation, IR absorption showed signature of water generation with broad absorption peak around 3386 cm^{-1} . There is a slight decrease in the 1736 cm^{-1} absorption, which may be connected to disintegration processes induced by radiation [4]. The aged sample, however, lost water and recovered the C=O concentration as depicted from the decrease in broad absorption peak around 3386 cm^{-1} and partial gain in 1736 cm^{-1} absorption.

Analogous results were obtained for Bayfol samples, irradiated with 1 MGy as illustrated in Fig. (7b). The loss of water (at 3386 cm^{-1}) as a result of sample aging slightly takes place. There are two stretching vibrations of C=O appears at 1791 cm^{-1} and 1754 cm^{-1} which belongs to symmetric and antisymmetric stretches of two adjacent carbonyl groups. These absorptions decrease further after aging the sample. Similarly do the 1598 cm^{-1} and 1514 cm^{-1} absorptions. The later results may be associated with formation and efflux of CO_2 gas through time or with late redox reaction occurred during the preservation time.

Conclusion

Aging of radiation-induced effects in polymeric material is a crucial factor for its long term performance of the material and compounds during and after exposure to radiation. The current results demonstrate the living effect of radiation; synthesized compounds in the polymeric material migrated through the material to the surface of the samples or exploit the available spaces among polymer fibers. These circumstances formed adhesive resin at the surface or soft fillings inside the fabric of the material during and after exposure. Possible accompanying chemical reactions may exist and associated with radiation synthesis. Cyclic and aromatic structures are more responsive to late radiation effects. Aging of radiation induced defects, hence, is another origin of radiation induced damage. The living effect of radiation has a considerable importance in radiation protection and dose calculation.

References

- 1- Elmaghraby, E. K., Seddik, U. Thermophysical properties and reaction kinetics of irradiated poly allyl diglycol carbonates nuclear track detector, *Radiat. Effects Defects Solids*, 170(7-8), 621–629.
- 2- Elmaghraby, E. K., Salama, T. A. (2010) Investigation of the fluorescence emitted from polyallyl diglycol carbonate modified by gamma-ray radiation excited by UV radiation, *Radiat. Effects Defects Solids*, 165 (4), 321–328(2015).
- 3- Salama, T. A. , Elmaghraby, E. K. High gamma-ray dose measurement using nuclear track detector, *Radiat. Protect. Dosimetry* 140 (3), 218–222(2010).
- 4- Elmaghraby, E. K. Radiation interaction with matter: An approach at the nanometer scale, in: B. I. Kharisov, O. V. Kharissova, U. O. Mendez (Eds.), *Radiation Synthesis of Materials and Compounds*, CRC Press, Taylor & Francis Group, pp. 403–422(2013).
- 5- Yamauchi, T., Nakai, H., Somaki, Y., Oda, K. (2003) Formation of CO_2 gas and OH groups in cr-39 plastics due to gamma-ray and ions irradiation, *Radiat. Meas.* 36 (16), 99 – 103(2003) .
- 6- Mori, Y., Yamauchi, T., Kanasaki, M., Hattori, A., Oda, K., Kodaira, S., Konishi, T., Yasuda, N., Tojo, S., Honda, Y., Barillon, R. Vacuum effects on the radiation chemical yields in PADC films exposed to gamma rays and heavy ions, *Radiat. Meas.* 50 (2013), 97 – 102(2013).
- 7- El-Saftawy, A., Reheem, A. A., Kandil, S., E. Aal, S. A., Salama, S. Comparative studies on PADC polymeric detector treated by gamma radiation and

- Ar ion beam, Appl. Surf. Sci. 371, 596 – 606(2016).
- 8- Zaki, M. F., Elmaghraby, E. K., Elbasaty, A. B. Structural alterations of polycarbonate/PBT by gamma irradiation for high technology applications, J. Adhesion Sci. Technol. 30 (4),443–457(2016).
 - 9- Elmaghraby, E.K. Resonant neutron-induced atomic displacements, Nucl. Instrum. Methods Phys. Res B, 398, 42-47(2017).
 - 10- Utracki, L.A., Wilkie, C.A. Polymer Blends Handbook, second edition, Springer Netherlands, ISBN 978-94-007-6063-9,978-94-007-6064-6(2014).
 - 11- American Society for Testing and Materials (ASTM) International Standard Test Method for Microindentation Hardness of Materials, ASTM E384-17 Standard (2017).
 - 12- Zaki, M. F., Elmaghraby, E. K. Photoluminescence of Irradiation Induced Defect on CR-39, Phil. Mag. 88(23), 2945- 2951(2008).
 - 13- Abdul-Kader, A. Surface modifications of PADC polymeric material by ion beam bombardment for high technology applications, Radiat. Meas. 69 (2014) 1 – 6(2014).
 - 14- Tayel, A. , Zaki, M., Basaty, A. E., Hegazy, T. M. Modifications induced by gamma irradiation to makrofol polymer nuclear track detector, J. Adv. Res. 6 (2), 219 – 224(2015).